Technical Report

TR-03-15

Reduction of uranyl carbonate and hydroxyl complexes and neptunyl carbonate complexes studied with chemical-electrochemical methods and rixs spectroscopy

Sergei Butorin, Uppsala University

Kaija Ollila, VTT Processes

Yngve Albinsson, Chalmers University of Technology

Joseph Nordgren, Uppsala University

Lars Werme, Svensk Kärnbränslehantering AB

October 2003

Svensk Kärnbränslehantering AB
Swedish Nuclear Fuel
and Waste Management Co
Box 5864
SE-102 40 Stockholm Sweden
Tel 08-459 84 00
+46 8 459 84 00
Fax 08-661 57 19
+46 8 661 57 19

Reduction of uranyl carbonate and hydroxyl complexes and neptunyl carbonate complexes studied with chemical-electrochemical methods and rixs spectroscopy

Sergei Butorin, Uppsala University

Kaija Ollila, VTT Processes

Yngve Albinsson, Chalmers University of Technology

Joseph Nordgren, Uppsala University

Lars Werme, Svensk Kärnbränslehantering AB

October 2003

Contents

1 Introduction

Sweden and Finland plan to dispose of spent fuel from commercial nuclear power plants in deep underground repositories sited in granitic rocks. The fuel assemblies will be placed in canisters consisting of an outer corrosion-resistant copper shell with an inner cast iron insert that gives mechanical strength and reduces void space in the canister. The canister will be placed in a disposal borehole lined with compacted bentonite blocks. After sealing of the borehole, groundwater seepage will saturate the bentonite. The water flow path and transport mechanism between the host rock and the canister will be via diffusion through the swollen bentonite. Any oxygen trapped in the repository will be consumed by reaction with the host rock, pyrite in the bentonite and through microbial activity, giving long-term conditions with low redox potentials. Under these conditions, uranium dioxide – the matrix of unirradiated fuel – is a stable phase.

This reducing near-field environment can upset by radiolysis of water caused by the radioactivity of the fuel, which after a few hundred years will be primarily alpha activity. Radiolysis of water produces equal amounts of oxidising and reducing species, but the reducing species produced by alpha radiolysis is molecular hydrogen, which is expected to be far less reactive than the produced oxidising species, H_2O_2. Alpha radiolysis could create locally oxidising conditions close to the fuel surface and oxidise the U(IV) in the uranium dioxide fuel to the more soluble U(VI) oxidation state. Furthermore, the solubility of U(VI) is enhanced in the presence of bicarbonate/carbonate by the formation of strong anionic uranyl carbonate complexes. This increase in solubility can amount to 4 to 5 orders of magnitude depending on the composition of the groundwater in contact with the fuel. The other tetravalent actinides in the fuel, Np and Pu, also have higher solubilities when oxidised beyond 4+ to neptunyl and plutonyl species.

Once these actinides have been mobilised through oxidation, they can migrate away from this potentially oxidising region and will encounter an oxygen free, reducing environment caused by the anaerobic corrosion of the cast iron insert. The actinyl species are no longer thermodynamically stable and reduction to the tetravalent state will be possible. There is, however, an open question whether the reduction kinetics will be sufficiently high to cause reduction in solution and if sorption onto the corroding iron surface will be accompanied by an electron transfer sufficiently rapid to reduce the actinide back to the tetravalent state.

This report contains the results of experimental studies of uranium reduction-depletion from water solutions in the presence of corroding iron and spectroscopic studies of the oxidation state of uranium and neptunium sorbed/precipitated onto iron under oxygen free conditions using resonant inelastic soft x-ray scattering (RIXS) spectroscopy.

The work reported here was performed as a part of the European Commission 5th Framework Programme under contract No. FIKW-CT-2000-0019.

2 Experimental, RIXS measurements

The RIXS measurements were performed on uranium and neptunium samples. VTT prepared the uranium samples and Chalmers Technical University (CTH) prepared the neptunium samples. Most of the RIXS measurements was performed at the Advanced Light Source at Lawrence Berkeley National Laboratory, USA. For the study of uranium, some measurements were also performed at the MAX-lab, Lund University, Lund, Sweden. The theoretical background to RIXS spectroscopy applied to strongly electron-correlated systems, such as the actinide complexes studied here is discussed in detail by Butorin /1/. It is beyond the scope of this report to discuss the spectroscopic technique itself. Only the results of the measurements will be discussed here.

2.1 Sample preparation, uranium samples

The method used by VTT was as follows. Iron foils were polished on one side with diamond spray (1 and 1/4 μm). An aliquot of U(VI) was added in the form of uranyl nitrate solution to deaerated modified Allard groundwater (100 ml) /2/ in a polyethylene bottle under N_2 atmosphere in a glove box. The composition of the Allard water is given in Table 2-1. The solution was allowed to equilibrate for a couple of hours. The starting concentration of uranium was about 500 ppb. At this uranium concentration, the dominating uranium species in solution are calculated to be $UO_2(CO_3)_3^{4-}$ (70%) and $UO_2(CO_3)_2^{2-}$ (25%). After equilibration, the Fe foils (2 pieces: 2 × 3 cm) were immersed in the solution in the bottle. The foils were placed on a small supporter (Teflon) the polished side upward. The experimental vessel was then allowed to stay tightly closed in the glove box.

The total U concentration in the solution was measured as a function of time with ICP-MS. The samplings were made without filtration. The redox potential (Eh) was measured after the experimental time of 40 days with gold as sensing electrode and a Ag/AgCl/3M KCl as reference electrode.

There was a rapid decrease in U concentration, see Figure 2-1. A black 'deposit' was observed on the surface of Fe foils after 3–4 weeks.

The measured redox potential in the solution at the end of the experimental period of 35 days was low, Eh= –450 mV.

The Fe foils that were sent for RIXS analyses had a reaction time of 17 days and 8.5 months. The U concentration in solution for the 17 days sample was 2.6×10^{-9} M. For the longer contact time, U concentration in solution was 1.5×10^{-10} M. The amount of black 'deposit' layer had increased.

Table 2-1. Composition of Allard water /2/.

	(mg/L)	(mmol/L)
Na^+	52.5	2.30
Ca^{2+}	5.1	0.13
Mg^{2+}	0.7	0.03
K^+	3.9	0.10
SiO_2	1.7	0.03
SO_4^{2-}	9.6	0.10
Cl^-	48.8	1.40
HCO_3^-	65.0	1.10
	$pH_{theoretical,\ log\ pCO2=\ -4}$	8.80

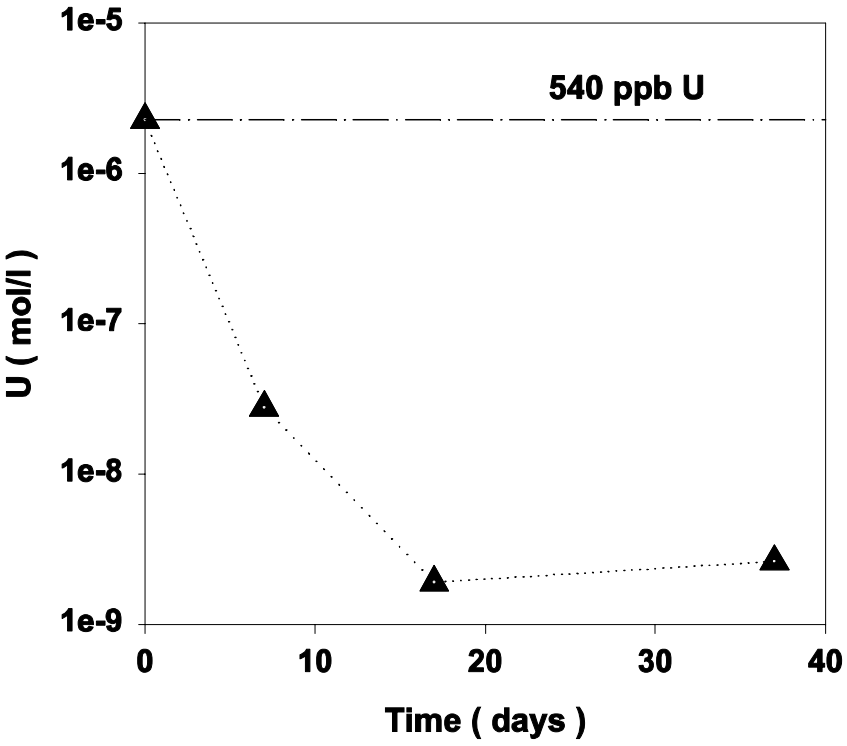

Figure 2-1. *U concentration in Allard groundwater in the presence of metallic iron (Fe foils).*

2.2 Sample preparation, neptunium samples

The method used by CTH was as follows. The iron plates, about 1 cm^2 in size, were glued to a PEEK-plate using either epoxy glue or silicon glue in order to avoid radioactive contamination on the reverse side of the iron plate. The plates were put in PEEK lined steel vessels that can function with an overpressure of gas inside. These will be referred to as pressure vessels in this report. Figure 2-2 shows a photograph of the components of this vessel as well as the assembled vessel. Approximately 50 Bq of pentavalent neptunium was added to 20 ml of Allard water (see Table 2-1). The resulting starting concentration of neptunium in solution was approximately 4×10^{-7} M. Before the start of the exposure, the solution and the pressure vessel were purged with hydrogen gas. After sealing the vessel, an overpressure of 50 bar of hydrogen gas was applied. The neptunium concentration in solution was monitored every week and after four weeks, when the residual amount was less than 1% (no measurable Np in solution), the iron plates were removed.

The dominating neptunium species in solution are calculated to be $NpO_2CO_3^-$ (75%) and NpO_2^+ (25%).

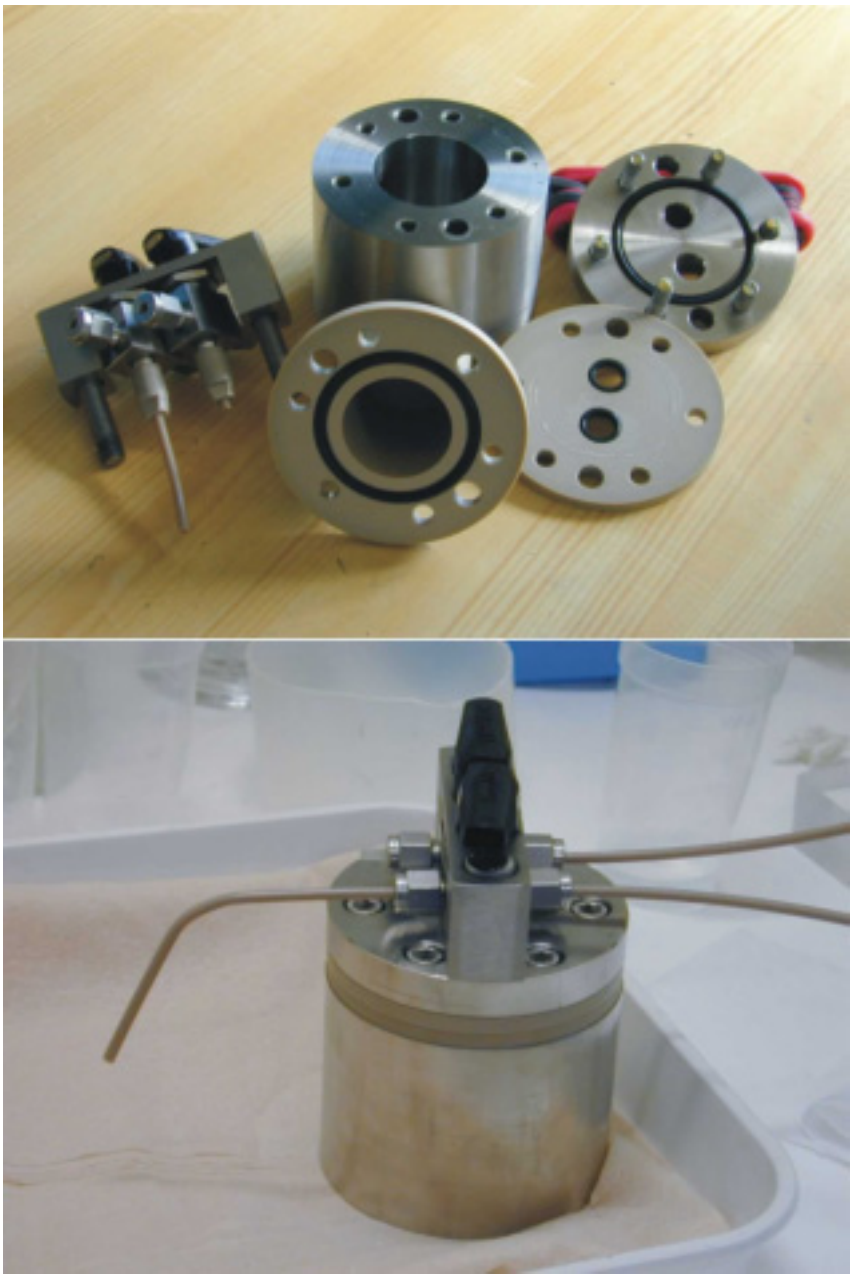

Figure 2-2. *Photographs of the components and the assembled pressure vessel used for preparing the neptunium samples for RIXS measurements.*

2.3 RIXS measurement

RIXS measurements at the U 5d threshold provide an opportunity to study in detail elementary excitations in U compounds due to the higher resolution of such experiments in comparison with those at the U 3d and 4d thresholds /1/. It has turned out that the technique is very sensitive to the valency and the chemical state of uranium in contrast to x-ray absorption spectroscopy (XAS). The 5d core-hole lifetime broadening is quite large, thus reducing the utility of XAS. As a result, the U 5d absorption spectra do not exhibit many sharp features /3/. The substantial smearing of the spectral structures hampers the analysis of the chemical state and the chemical environment of uranium in various compounds. In particular, it is difficult to distinguish between uranium species with different oxidation states, especially in the case when one of species has a much lower concentration than another. In this situation, the virtually unlimited resolution (defined by the response function of the instrument) of the RIXS technique and its ability to enhance transitions to low-lying excited states are especially useful. RIXS spectroscopy provides good signatures in terms of new distinct transitions, representing electronic excitations within the 5f shell and having a characteristic profile for U(IV). The same kind of RIXS measurements were also made for the Np-on-Fe sample prepared at the CTH. The spectra were recorded at energies of the incident photon beam set to the pre-threshold structure in the Np 5*d* x-ray absorption spectrum.

The experiments were performed at undulator beamline 7.0 of the Advanced Light Source (ALS), LBNL, employing a spherical grating monochromator /3/. Resonant ultra-soft x-ray scattering spectra from the samples were recorded using a grazing-incidence grating spectrometer /4/ with a two-dimensional detector. The incidence angle of the photon beam was approximately 15º from the sample surface and the spectrometer was placed in the horizontal plane at an angle of 90º with respect to the incidence beam. The bandwidth of the excitation was about 65 meV. The elastic peak the total energy resolution of the RIXS data was estimated from the full width at half maximum of to be 160 meV.

3 Results and discussion, RIXS measurements

3.1 Uranium

Previous measurements on a set of model uranium compounds and companion model calculations /3/ showed that setting the energy of the incident beam close to the U 5d thresholds enhances the inelastic scattering cross section and ensures that electronic states of 5f symmetry are probed according to dipole selection rules. The spectral contribution of intra-ionic f-f transitions of U is enhanced at excitation energies close to 100 eV while at higher energies of the incident photon beam set to the main 5d absorption edge (e.g. 115 eV) inter-ionic excitations of charge-transfer character, such as ligand 2p – U 5f charge-transfer, dominate the RIXS spectra. The spectral pattern of intra-ionic f-f excitations is mainly determined by the formal valency of U, in turn, the charge-transfer transitions strongly depend on the chemical environment of U ions.

Figure 3-1 displays a set of scattering data from the Fe sample with 17-day exposure recorded at the incident x-ray energy of 100 eV, which corresponds to the energy of the weak pre-threshold structure in the U 5d x-ray absorption spectrum. A series of spectra were randomly measured from different 1 mm × 150 µm areas on the Fe sample surface. Six of them are shown in the figure along with spectra of the reference oxides UO_2 and UO_3 that contain U(IV) and U(VI), respectively. The choice of the excitation energy is defined by the necessity to selectively look at the intra-ionic f-f transitions.

An inspection of Figure 3-1 shows the presence of two distinct RIXS structures at energy losses of about – 0.8 and –1.15 eV in the UO_2 spectrum. These structures represent f-f transitions as incident x-rays are inelastically scattered on electronic excitations within the 5f shell. The structures are very well reproduced by model calculations of RIXS spectra using atomic multiplet theory for the U(IV) ion. Naturally, these structures are absent in the UO_3 spectrum due to the formal $5f^0$ configuration of the U(VI) ions. In this situation, any reduction of U(VI) on the Fe surface should result in the appearance of characteristic RIXS structures. The present measurements indeed reveal the presence of a significant inelastic contribution in spectra recorded from some areas (spectra #4–6) on the surface of the Fe sample, thus indicating U(VI) reduction in those areas.

However, a comparison of RIXS spectra of the charge-transfer transitions between the foil and UO_2, made in Figure 3-2, suggests that the U(IV) species on the Fe foil are not necessarily in the form of uranium dioxide. The RIXS profiles of the compared spectra are somewhat different. Similar results were obtained for another Fe foil prepared under the same conditions but with much longer exposure (8.5 month) to the U(VI) solution.

Quantitative estimates of the amount of reduced uranium were made by normalizing the recorded spectra to the characteristic core-to-core fluorescence lines and by comparison to model oxide systems with well-defined oxidation states for uranium. Using UO_2 single crystal standards, we were able to compare the recorded spectra from the standards and the samples described above after normalization to the non-resonant U 6p-to-5d fluorescence line recorded with excitation above the 5d edge. An example of such a comparison is shown in Figure 3-3. By fitting the elastic peak with the Voigt profile and estimating the area under the spectral curve in the energy-loss range corresponding to the f-f transitions the amount of reduced uranium can be derived. In this manner, we could estimate that 73% of the total uranium on the foil from the 17 days experiment is in fact present as U(IV) and for the 8.5 months experiment 42% was present as U(IV) taking into account the spatial heterogeneity. The reason for this reversed behaviour may be possible peeling off of ayers of the U(IV) compound.

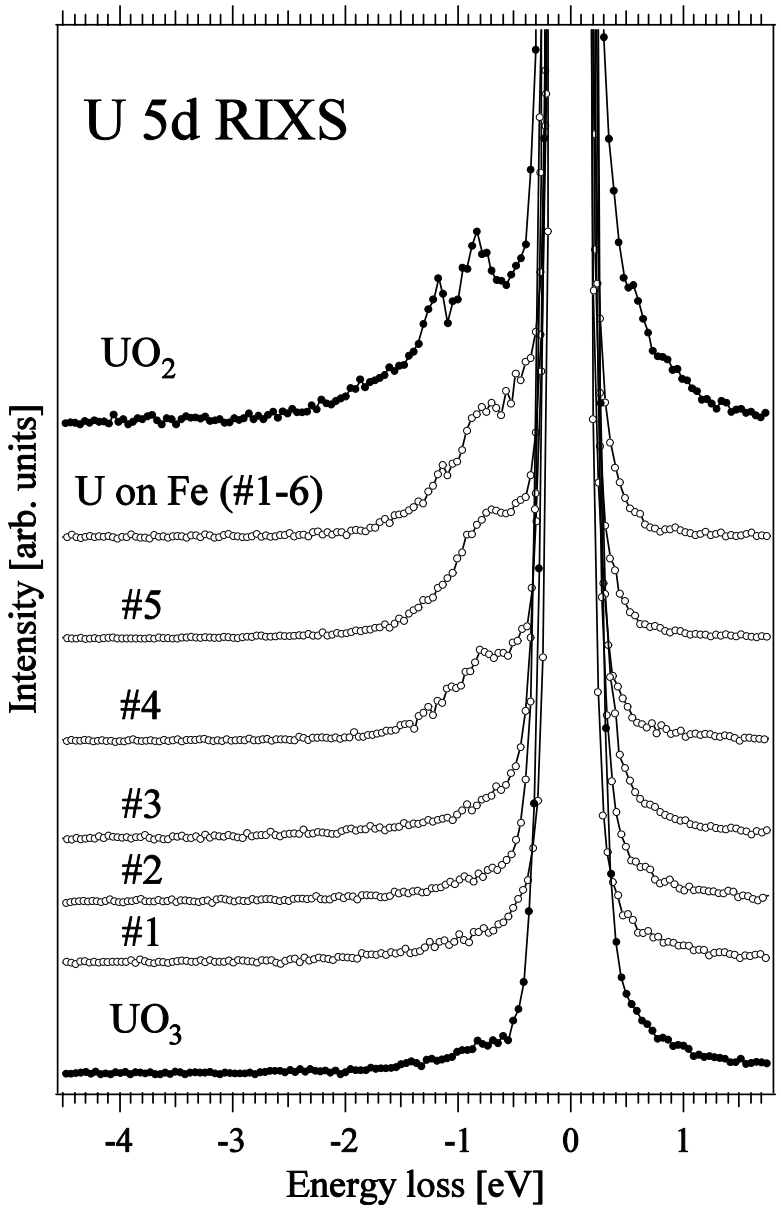

Figure 3-1. *Enhanced inelastic part of soft x-ray scattering spectra of UO_2, UO_3 and U adsorbed on the Fe foil (elastic peaks are at 0 eV). The energy of the incident photons was set to 100 eV. The six spectra of adsorbed U were randomly measured from different 1 mm × 150 μm areas on the surface of the Fe sample.*

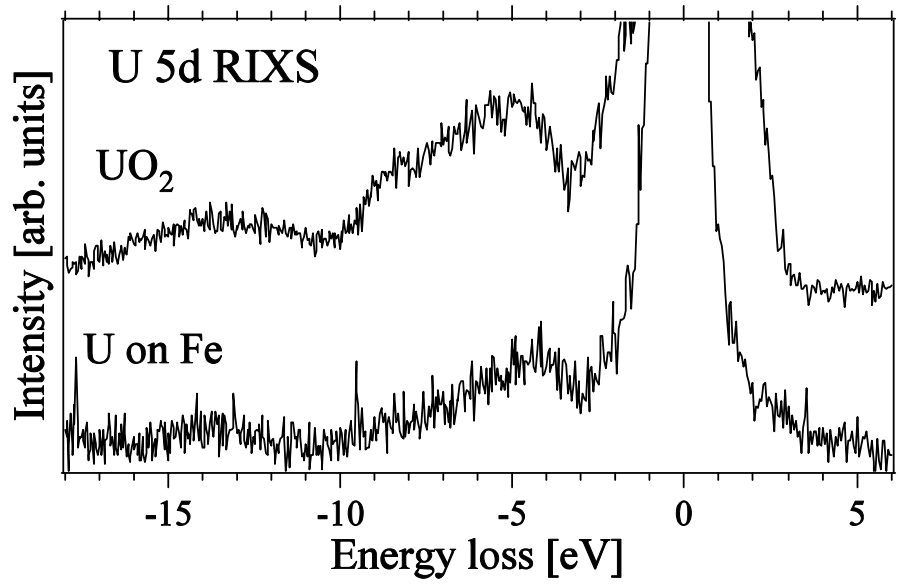

Figure 3-2. *Enhanced inelastic part of the soft x-ray scattering spectra of UO_2 and U adsorbed on the Fe foil recorded at the excitation energy of 115.0 eV.*

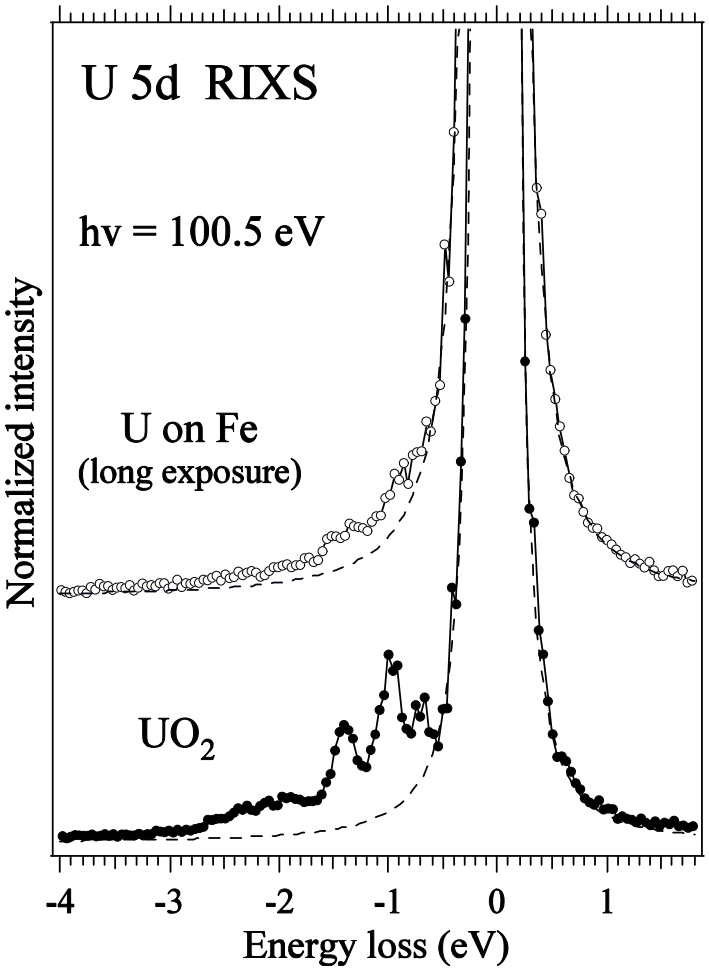

Figure 3-3. *Enhanced inelastic part representing f-f excitations in the soft x-ray scattering spectra of single-crystal UO_2 and U on the long-exposure Fe sample. Dashed lines represent Voigt fits of the elastic peaks.*

3.2 Neptunium

Figure 3-4 shows a number of RIXS spectra of NpO_2 used as a reference for the tetravalent system with the defined oxidation state for Np. The spectra were recorded at energies of the incident photon beam set to the pre-threshold structure in the Np 5*d* x-ray absorption spectrum. (The top figure in Figure 3-4.) At such energies, the x-ray scattering cross-section is enhanced for *f-f* transitions. The excitation energies for the spectra are indicated in the figure with the letters a, b, c, and d. The energy losses of the corresponding RIXS structures observed in Figure 3-4 are in agreement with optical absorption measurements of *f-f* transitions in Np(IV) systems /5, 6/.

The spectra in Figure 3-4 are compared with the results from atomic multiplet calculations for the Np(IV) ion. The calculations were performed in a similar manner as was described for the case of U(IV) in the previous section, only this time the $F^k(5f; 5f)$ integrals were scaled down to 70%. The initial and final states of the scattering process were taken to be those of the $5f^3$ configuration with the intermediate states of $5d^9 5f^4$ character which are mainly autoionized to $5f^2\ g$ states. The calculated spectra show slight differences in the energy position for some RIXS structures when compared with the experimental spectra. This is likely due to the influence of the crystal field interaction and/or the Np 5*f*-O 2*p* hybridization, which were not taken into account in the calculations. The extra-structure observed in the experimental spectra at an energy loss of around 950 meV may also be a result of the crystal field interaction. Nevertheless, the present calculations account for the overall RIXS profile and behaviour and reproduce its dependence on the excitation energy.

Figure 3-5 displays RIXS spectra of Np sorbed on the Fe stripe along with NpO_2 spectra recorded at the same excitation energies. An inspection of this figure shows that the RIXS structures of both samples closely resemble each other. This resemblance unambiguously indicates the existence of Np in the form of Np(IV) on the studied Fe stripe.

RIXS spectra of the charge-transfer transitions between the foil and NpO_2 are shown in Figure 3-6. The corresponding spectra for uranium suggested that U(IV) species on the Fe foil is not necessarily in the form of uranium dioxide. The RIXS profiles of NpO_2 and neptunium on the iron are much more similar, indicating the Np(IV) species is likely to be NpO_2.

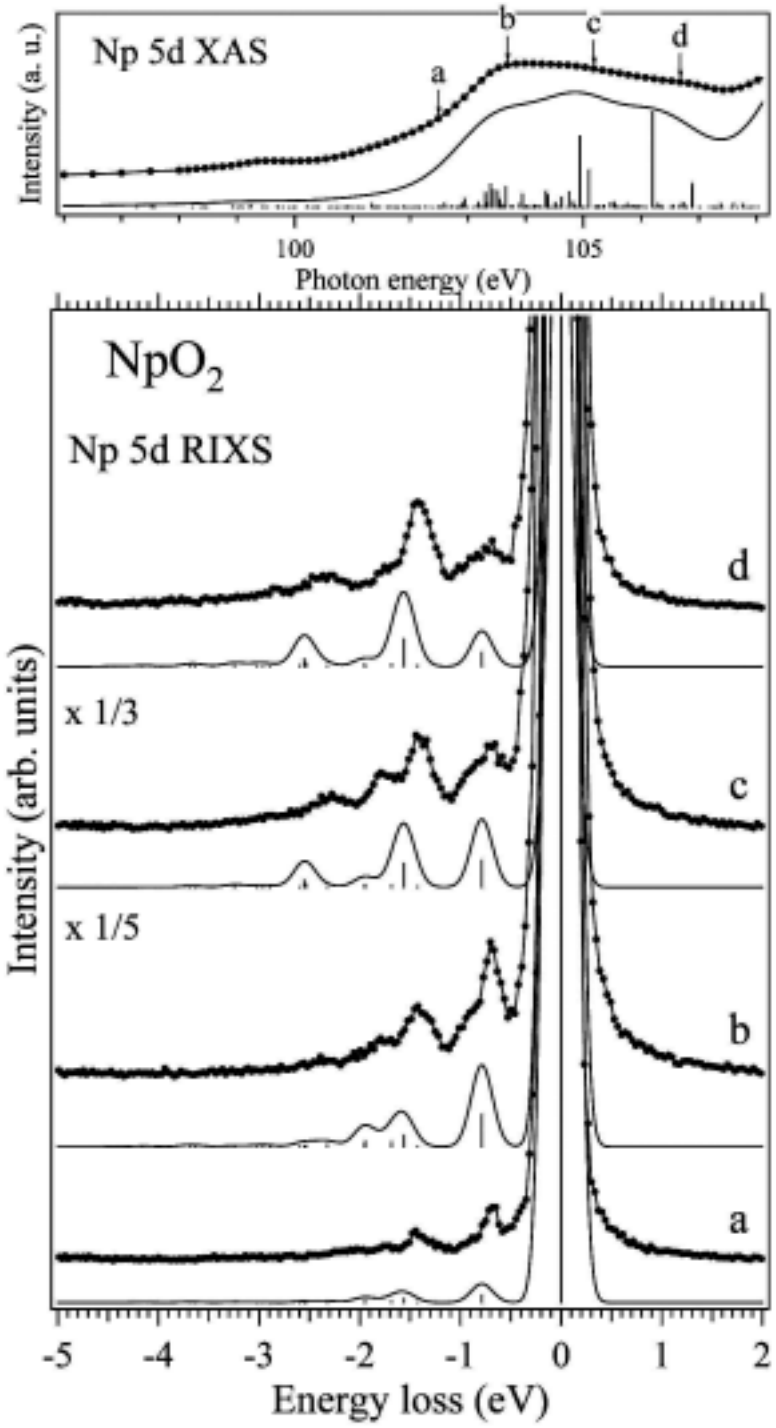

Figure 3-4. *Resonant x-ray scattering spectra of NpO2 recorded at different excitation energies close to the Np 5*d *threshold (lines with markers) together with the results of atomic multiplet calculations (sticks with thin lines) for the Np4+ ion. Excitation energies are indicated by arrows on the total electron yield spectrum at the Np 5*d *absorption edge shown in the top panel.*

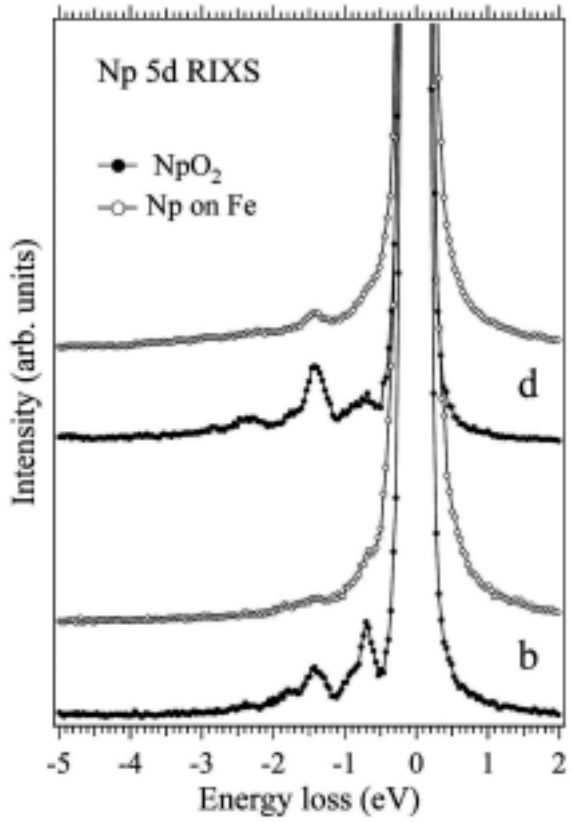

Figure 3-5. *Comparison of resonant inelastic soft x-ray scattering spectra of Np sorbed on the Fe stripe and NpO_2. Letters correspond to the same excitation energies as in Figure 3-4.*

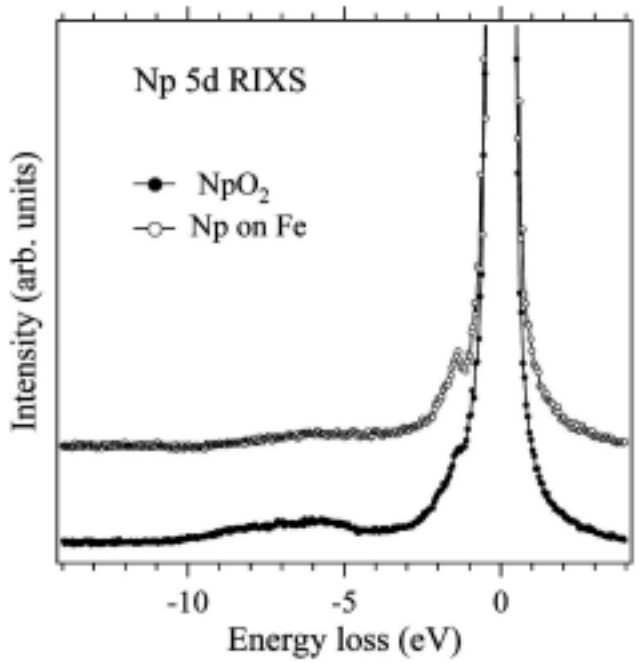

Figure 3-6. *RIXS spectra of the charge-transfer transitions between the iron foil and NpO_2.*

4 Experimental, chemical and electrochemical measurements

The species to be studied were U(VI) carbonates and U(VI) hydroxides. The solution for U(VI) carbonate complexes was a NaCl-$NaHCO_3$ solution. The dominant species under these conditions are $UO_2(CO_3)_3^{4-}$ (63%) and $UO_2(CO_3)_2^{2-}$ (24%). The NaCl-$NaHCO_3$ had an ionic strength (I = 0.003) and bicarbonate content (1.1 mM) similar to Allard groundwater. The U(VI) was added to solution as an aliquot of uranyl nitrate solution ($UO_2(NO_3)_2 \times 6\ H_2O$).

The solution for U(VI) hydroxide complexes was 0.1 M NaCl with high pH. The dominant species is $UO_2(OH)_3^-$ (99%).

Reduction tests were performed in the active corrosion cell under anaerobic conditions in the glove box (N_2). The cell was made of glass. It had an inner vessel made of polyethylene. Iron strips were immersed in deaerated U(VI) solution in the cell. The evolution of uranium concentration was followed versus reaction time with periodic sampling through the sampling port for further analysis of uranium (ICP-MS). The oxidation state of uranium in solution was analysed in selected tests using a method that is based on the separation of the tetravalent and hexavalent states by anion-exchange chromatography in HCl medium. The analyses of the U contents of each of the fractions were measured by ICP-MS. The method is described in detail elsewhere /7/.

The cell had electrodes for the in-situ monitoring of pH, E_h and corrosion potential of iron during reduction reaction /8/:

- palladium black electrode (hydrogen electrode) for pH,
- gold electrode for Eh,
- iron electrode for corrosion potential,
- silver-silver chloride electrode as reference.

The Fe electrode was made of iron metal of the same composition as the iron strips that were used as reducing agent in the aqueous phase.

The functioning of the pH and the reference Ag/AgCl electrodes caused problems in the preliminary measurements in NaCl-$NaHCO_3$. The potential values of all three electrodes changed from negative to positive 85 minutes after the start of a reduction test, Figure 4-1. Since the potential values changed simultaneously it was concluded that it was the potential of the reference electrode that had changed. After the test, the potential of the Ag/AgCl electrode was measured versus a commercial calomel electrode. The reading was not stable. One possible reason for failure could be the dissolution or cracking of the silver chloride coating of the electrode in the test solution that contained chloride ions. The lifetime of the Pd black electrode proved to be short, 4–5 days after the electrolysis, under anaerobic conditions.

After that, the reference and pH electrodes were replaced with commercial electrodes (Innovative Instruments, Inc. USA), which were made suitable for the corrosion cell. The leak-free Ag/AgCl reference electrode was constructed from PEEK. The filling electrolyte was 3.4 M KCl. The electrode has a junction that is highly conductive but not porous. The pH sensitive tube with a metal-metal oxide pH sensing mechanism was also constructed from PEEK.

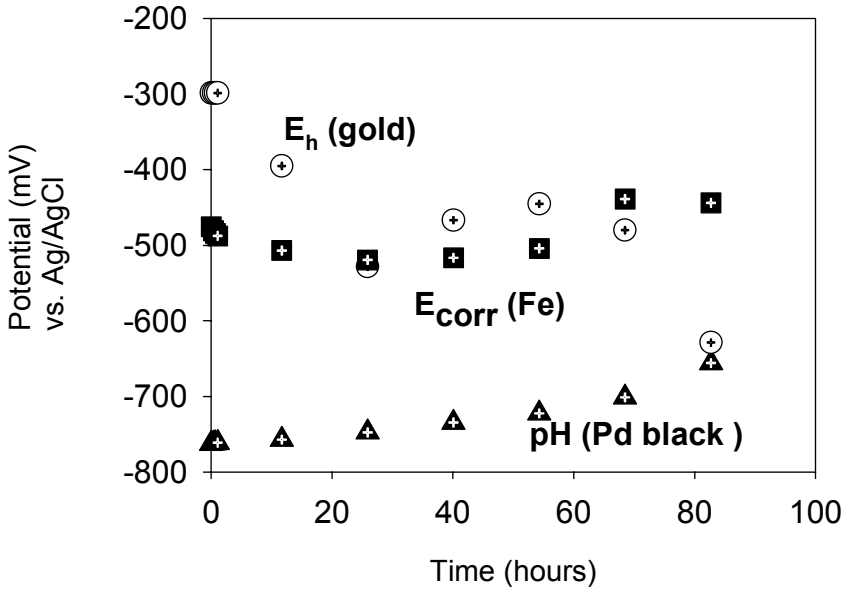

Figure 4-1. *Potential of pH, gold and Fe electrodes in a preliminary U reduction test in $NaCl$-$NaHCO_3$ solution (25°C).*

5 Results and discussion, chemical and electrochemical measurements

Two parallel reduction tests (Test I, II) were performed in NaCl-$NaHCO_3$ solution. The conditions are given in Table 5-1. The amount of iron was different in the tests. Otherwise the conditions were similar. The iron strips were transferred to test solution one day before the U addition. The temperature in the glove box was 30°C instead of the normal 25°C during these tests due to the breakdown of the cooling system of the box.

Table 5-1. Conditions of the reduction tests.

	Initial U (ppb)	Solution (ml)	Initial pH	Fe SA/solution V
Test I	560	300	8.7	19 cm^2/300 ml
Test II	500	250	8.7	38 cm^2/250 ml

The results of monitoring the pH, E_h and corrosion potential of iron in NaCl-$NaHCO_3$ in the presence of iron strips during the first 17 hours are shown in Figure 5-1 to Figure 5-6. The pH behaved somewhat differently in the tests (Figures 5-1 and 5-2). It is not known if this was dependent on the calibration of the electrode. The pH in Test I seems too low. The final pH (9.1) in Test II is in agreement with the measurements done in WP1 tests in Allard groundwater. The E_h was decreased to around – 400 mV due to the anaerobic corrosion of the iron surface, leading to the release of Fe^{2+}-ions to the solution. It was 50 mV lower at the end of the measurement period in Test II that had a higher ratio of the Fe surface to solution volume (Figures 5-3 and 5-4). There was some disturbance at the early stage of the measurement in Test II. The corrosion potential of iron stabilized in 3–4 hours at –530 mV.

After the addition of the U(VI), an aliquot of uranyl nitrate solution, the pH decreased slowly in Test I and more rapidly in Test II (Figures 5-7 and 5-8). There was a small initial increase in Test I. The pH started to increase again after 5 hours in Test II with more metallic iron. The E_h of the solution increased rapidly after the uranyl, UO_2^{2+}, addition. The reaction seemed to be very fast in Test II. At the later stages the Eh decreased to the original level again. The initial increase suggests the reaction between Fe^{2+} and U(VI)-carbonate complexes in solution, leading to the oxidation of Fe^{2+}. An attempt was made to analyse the oxidation state of the U in solution in Test I. The samples for the analyses were taken 3, 27 and 49 hours after the U addition, Table 5-2.

Table 5-2. Results for U oxidation state in solution.

Samples	U(IV) %	U(VI) %
3 hours	16	84
27 hours	51	49
49 hours	53	47

The results (Table 5-2) showed the presence of the U at the tetravalent state in solution. This suggests the reduction of U to take place in solution. The corrosion potential of the iron electrode remained approximately at the same level as before the U addition (Figures 5-11 and 5-12).

The evolutions of the total U contents in both tests are shown in Figures 5-13 and 5-14. In test I, there was a rapid decrease in U concentration during the first five hours after the U addition, which was followed by a slower decrease. The U decreased from 560 to 150 ppb with the reaction time of 55 hours under these conditions. In test II, the decrease was much faster, probably due to the larger amount of metallic iron (Table 5-1). The U decreased to 0.02 ppb (8.4×10^{-11} M), that is the detection limit of U by ICP-MS, with the reaction time of 24 hours. This U level is in agreement with the U concentrations measured in the isotope dilution tests of WP1 and WP2.

The reduction tests in 0.1 M NaCl (pH 11) were performed in the active corrosion cell equally with the tests in NaCl-$NaHCO_3$. The pH of the deaerated 0.1 M NaCl solution was adjusted to 11 with 0.1 M NaOH. The solution was allowed to equilibrate with the iron strips for one day before the U addition. The temperature in the glove box was 25°C during these tests. Two parallel tests were performed, Table 5-3.

Table 5-3. Conditions of the reduction tests in 0.1 M NaCl.

	Initial U (ppb)	Solution (ml)	Initial pH	Fe SA/V
Test III, IV	500	250	11.0	28 cm^2/200 ml

The pH electrode of the corrosion cell showed some inconsistency in the measurements; see Figures 5-15 and 5-16, which give the pH vs. time after the addition of the Fe metal to solution. The pH decreased slowly in both tests. The pH was checked with a Ross combination glass pH electrode at the end of the equilibration periods with iron strips by taking samples for measurements. According to these measurements, the pH had not changed from the original value of pH 11 in either of the tests. The potentials of gold and iron stabilized rapidly at low levels after the addition of the iron strips (Figures 5-17 and 5-18).

After the addition of the U(VI), an aliquot of uranyl nitrate solution, the continuous pH measurement in the reaction cell gave a falling value up to the end of the experimental time, see Figure 5-19, which shows the pH vs. time for Test III. This is in disagreement with the results of the parallel test, Figure 5-20. In this case the pH was measured with a micro-combination glass pH electrode by taking samples from the reaction cell. The measurements did not show any change in pH. The pH measurement with the Ross glass pH electrode at the end of the Test III gave also the original value of 11. It is probable that the pH does not change during the tests.

The E_h increased in Test III rapidly after the U addition from the level before the addition (~ –460 mV, Figure 5-17) and stayed higher after that, see Figure 5-21, suggesting the reaction between Fe^{2+} in solution and U(VI)-hydroxide complexes. There were disturbances in the measurement at the early stages of the test. The Eh decreased to the original level afterwards, in agreement with the reduction tests of uranyl carbonate. The parallel test gave a different result (Figure 5-22). The E_h stayed at the higher level to the end of the experimental time. The corrosion potential of iron did not change after the U addition in the tests (Figures 5-23 and 5-24).

The evolutions of the total U contents are shown in Figure 5-25. The test IV was continued for a longer period (8 days) in order to see the final U concentration. The U concentration decreased from 500 to 20 ppb in the presence of iron strips. The oxidation state of U was analysed in Test III. The samples were taken 2.5, 28 and 74 hours after the U addition. The amount of the U at the tetravalent state was lower than in the reduction tests I and II, see Table 5-4.

Table 5-4. Results for U oxidation state in solution.

Samples	U(IV) %	U(VI) %
2.5 hours	4	96
28 hours	12	88
74 hours	14	86

6 Figures, chemical and electrochemical measurements

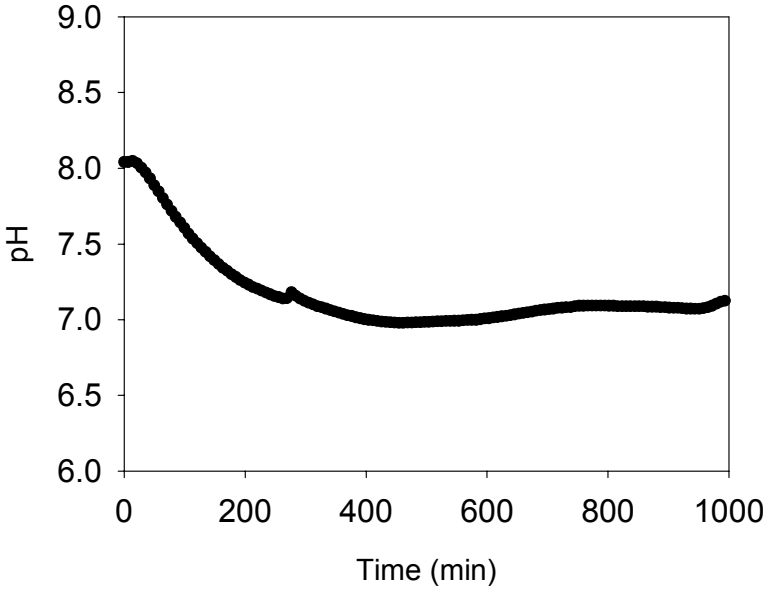

Figure 5-1. *pH in Test I after the addition of the iron strips to NaCl-$NaHCO_3$ solution (30°C).*

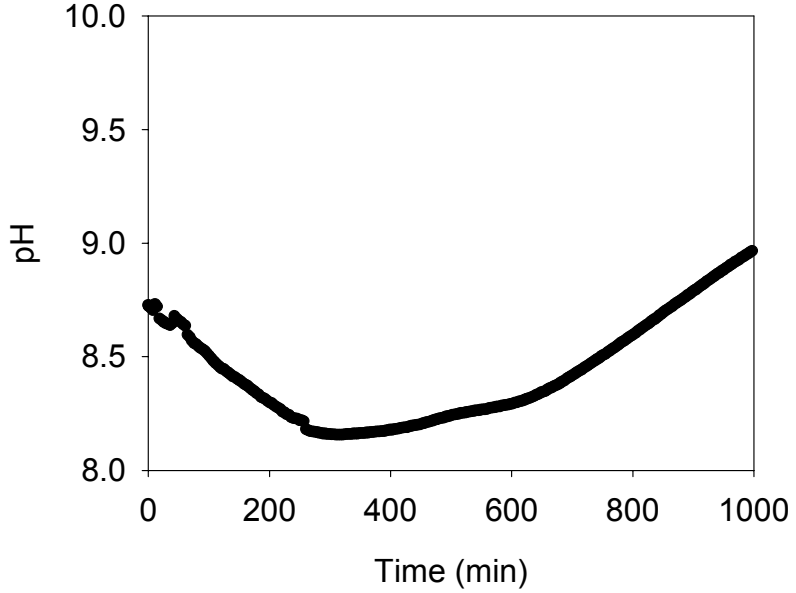

Figure 5-2. *pH in Test II after the addition of the iron strips to NaCl-$NaHCO_3$ solution (30°C).*

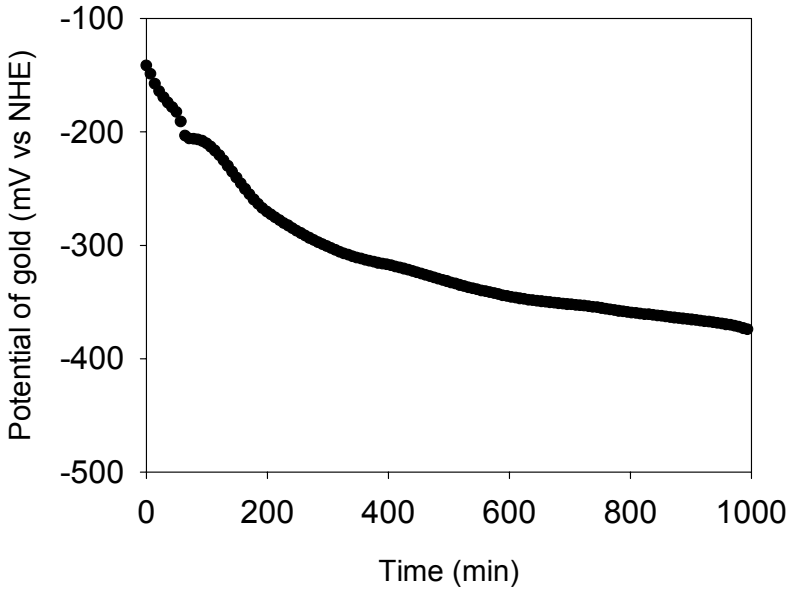

Figure 5-3. *E_h in Test I after the addition of the iron strips to NaCl-$NaHCO_3$ solution (30°C).*

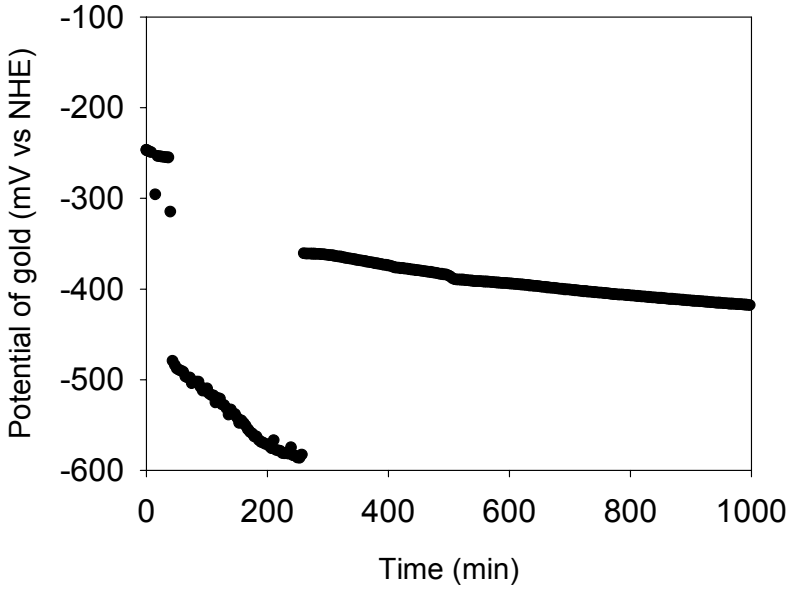

Figure 5-4. *E_h in Test II after the addition of the iron strips to NaCl-$NaHCO_3$ solution (30°C).*

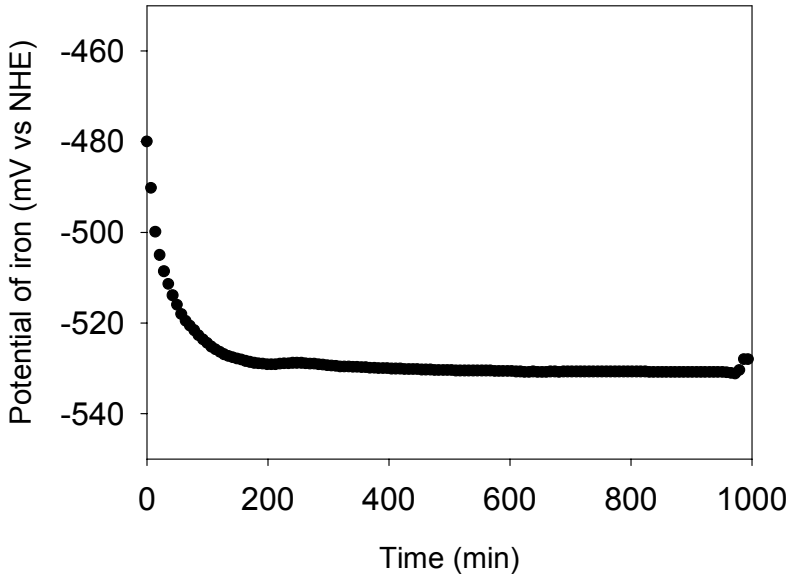

Figure 5-5. *Corrosion potential of iron in Test I after the addition of the iron strips to NaCl-$NaHCO_3$ solution (30°C).*

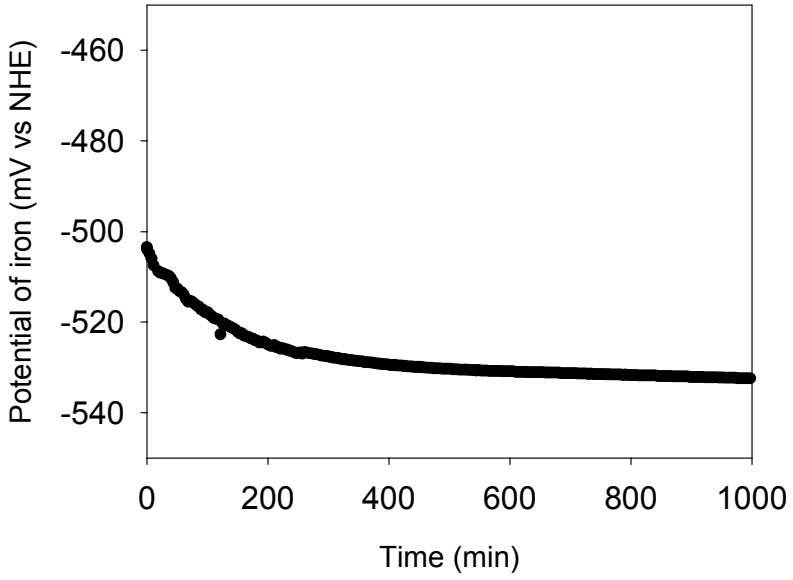

Figure 5-6*. Corrosion potential of iron in Test II after the addition of the iron strips to NaCl-$NaHCO_3$ solution (30°C).*

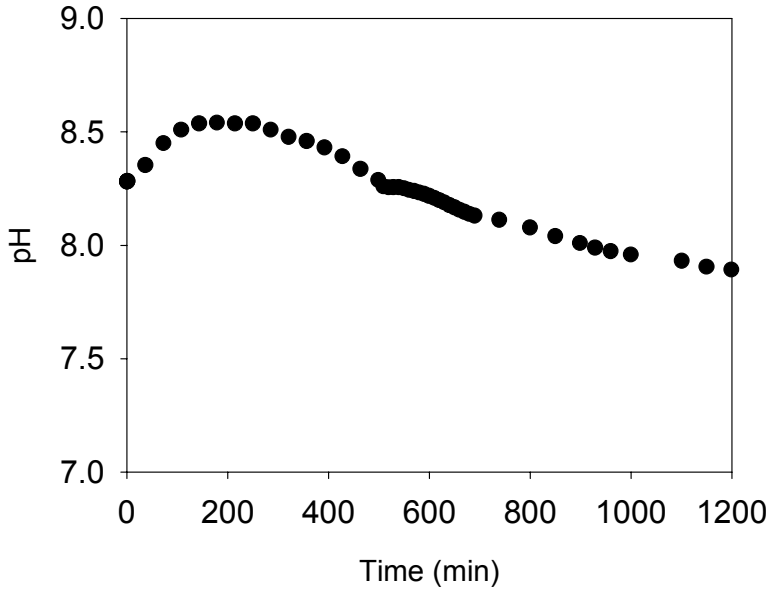

Figure 5-7*. pH in Test I after the addition of U to NaCl-$NaHCO_3$ solution in the presence of iron strips (30°C).*

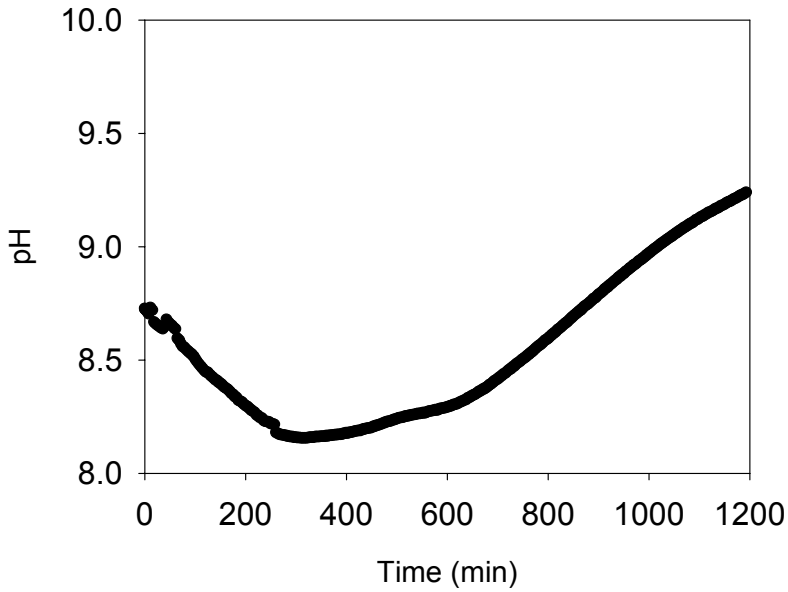

Figure 5-8. *pH in Test II after the addition of U to NaCl-$NaHCO_3$ solution in the presence of iron strips (30°C).*

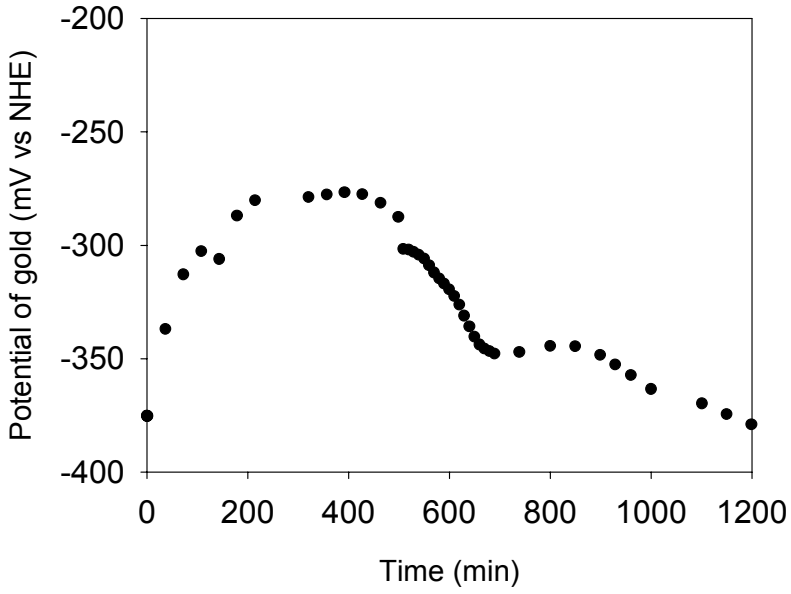

Figure 5-9. *E_h in Test I after the addition of U to NaCl-$NaHCO_3$ solution in the presence of iron strips (30°C).*

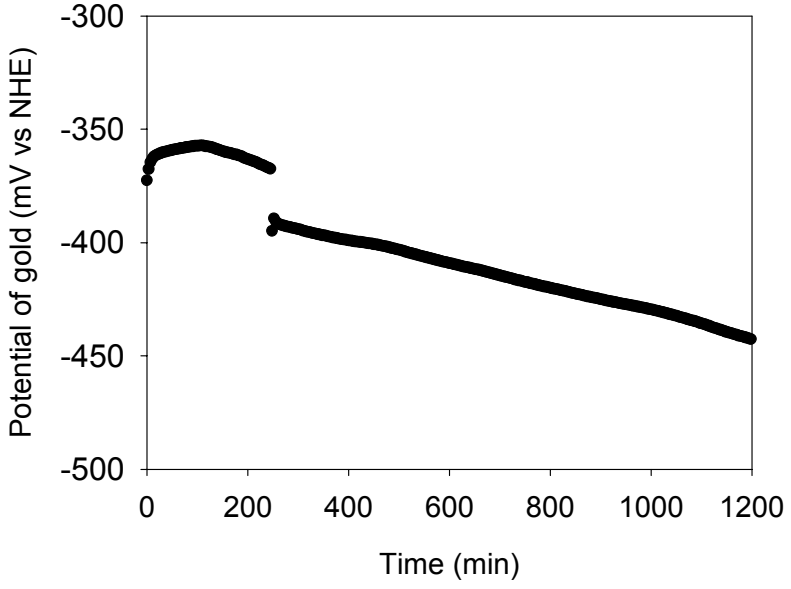

Figure 5-10. *E_h in Test II after the addition of U to NaCl-$NaHCO_3$ solution in the presence of iron strips (30°C).*

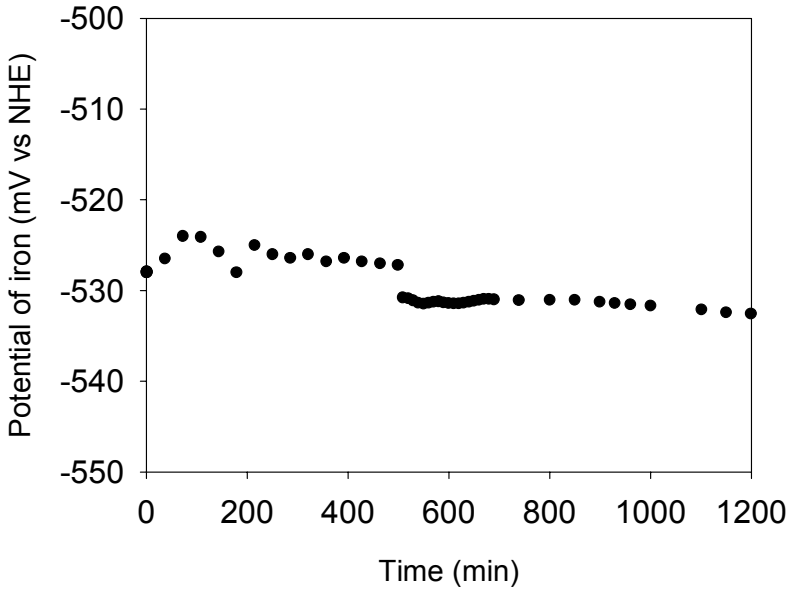

Figure 5-11. *Corrosion potential of iron in Test I after the addition of U to NaCl-$NaHCO_3$ solution in the presence of iron strips (30°C).*

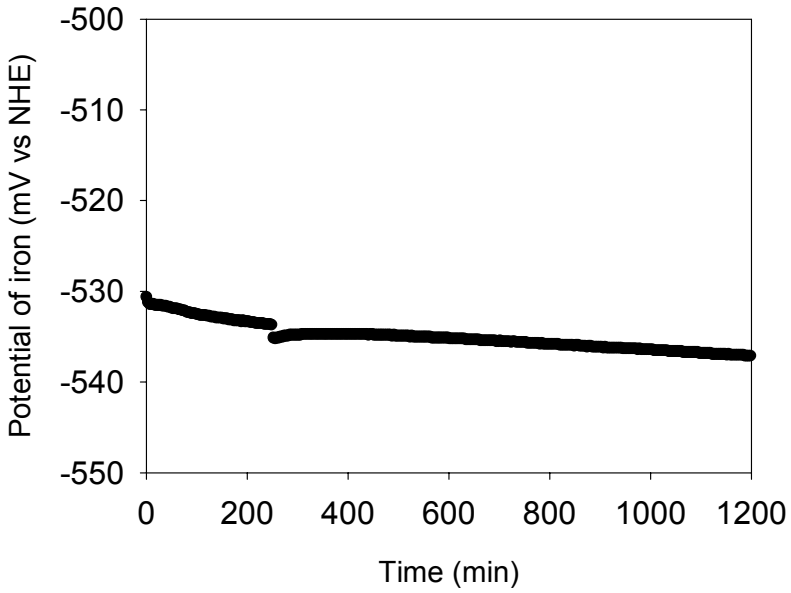

Figure 5-12. *Corrosion potential of iron in Test II after the addition of U to NaCl-$NaHCO_3$ solution in the presence of iron strips (30°C).*

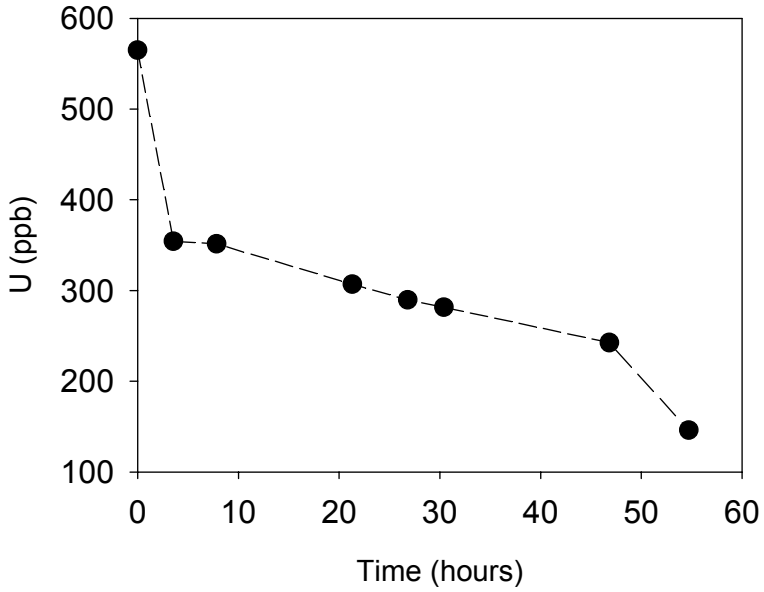

Figure 5-13. *Total U concentration (ppb) in Test I after the addition of U to NaCl-$NaHCO_3$ solution in the presence of iron strips (30°C).*

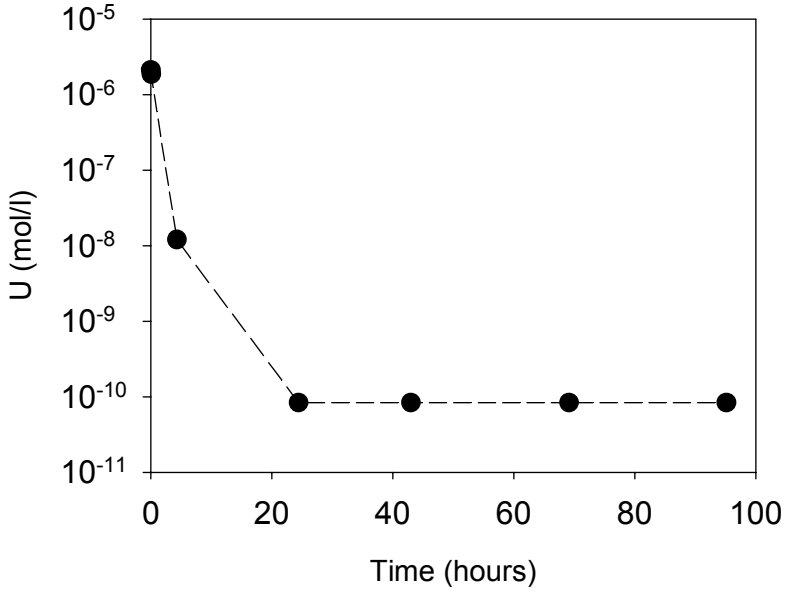

Figure 5-14. *Total U concentration (mol/l) in Test II after the addition of U to NaCl-$NaHCO_3$ solution in the presence of iron strips (30°C).*

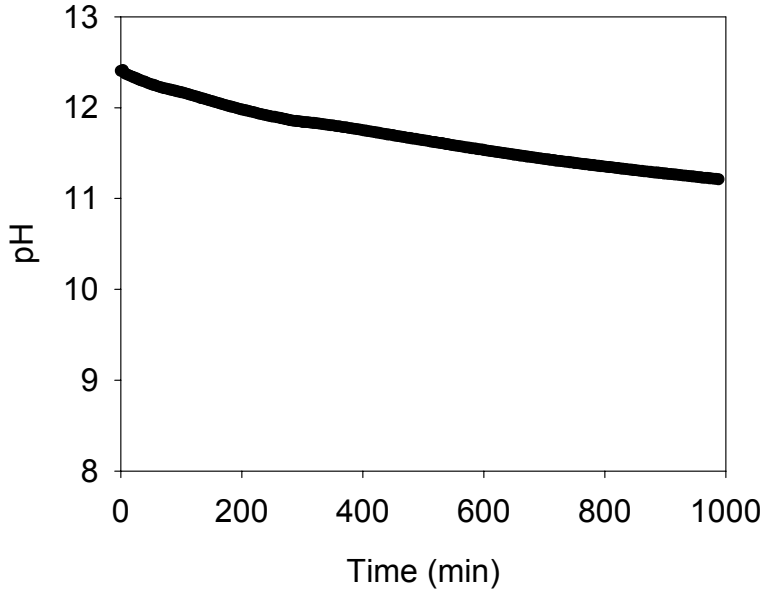

***Figure 5-15**. pH in Test III after the addition of the iron strips to 0.1 M NaCl, initial pH 11 (25°C).*

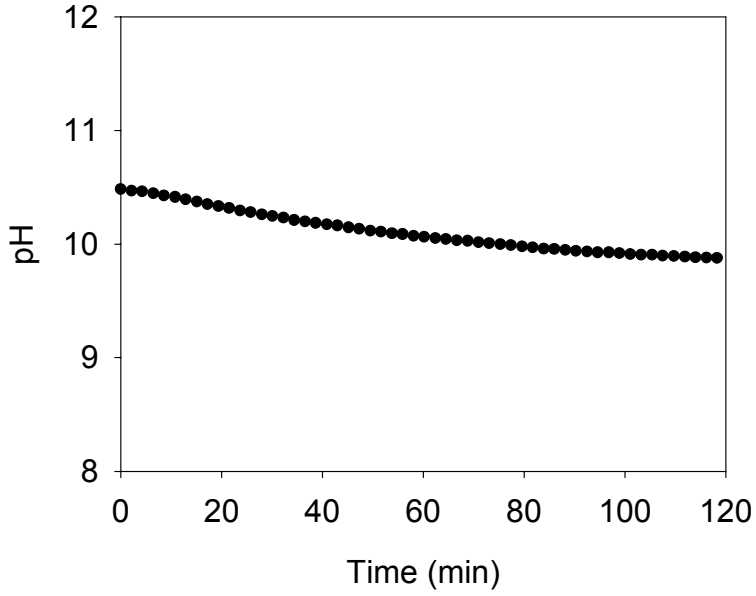

***Figure 5-16**. pH in Test IV after the addition of the iron strips to 0.1 M NaCl, initial pH 11 (25°C).*

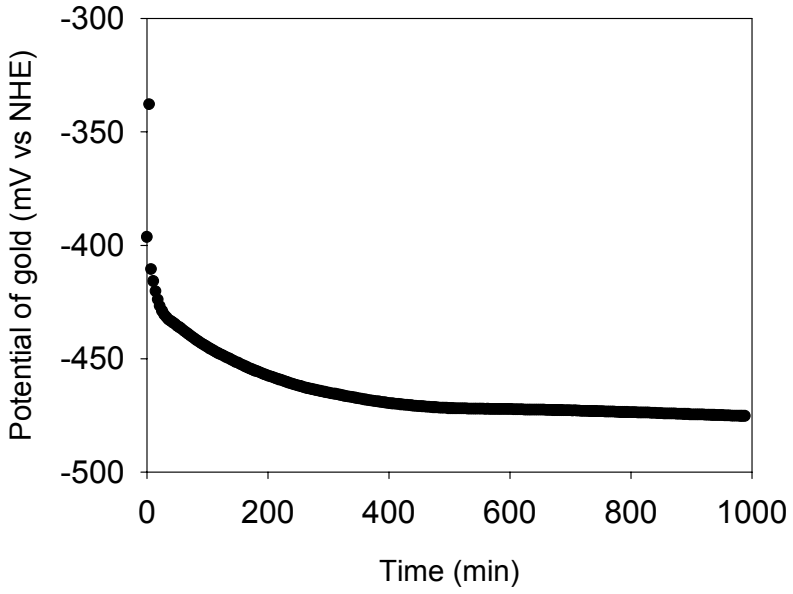

Figure 5-17. *E_h in Test III after the addition of the iron strips to 0.1 M NaCl, initial pH 11 (25°C).*

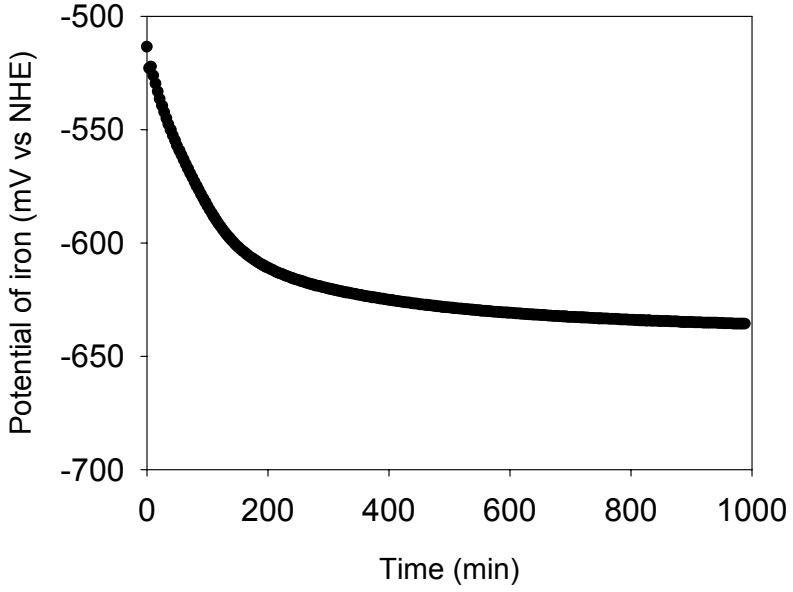

Figure 5-18. *Corrosion potential of iron in Test III after the addition of the iron strips to 0.1 M NaCl, initial pH 11 (25°C).*

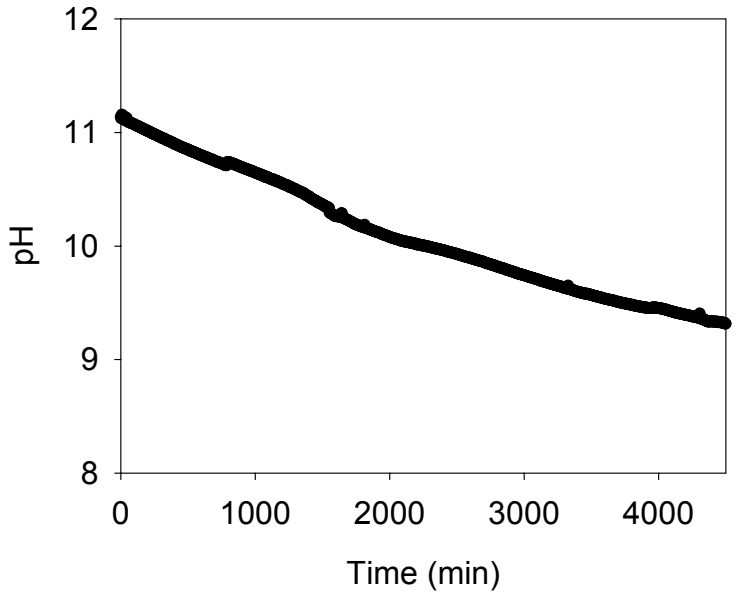

Figure 5-19. *pH in Test III after the addition of U to 0.1 M NaCl (initial pH 11) in the presence of iron strips (25°C).*

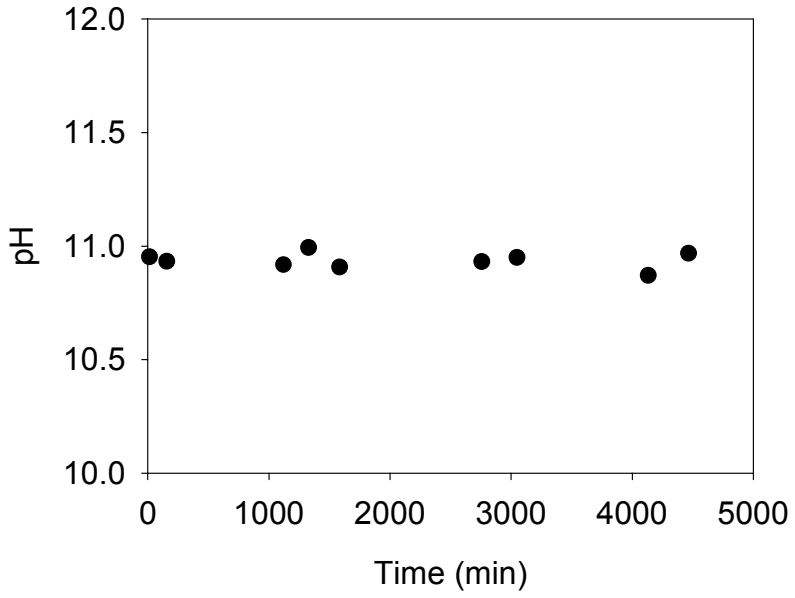

Figure 5-20. *pH in Test IV after the addition of U to 0.1 M NaCl (initial pH 11) in the presence of iron strips (25°C). The pH was measured with the help of samplings from the corrosion cell.*

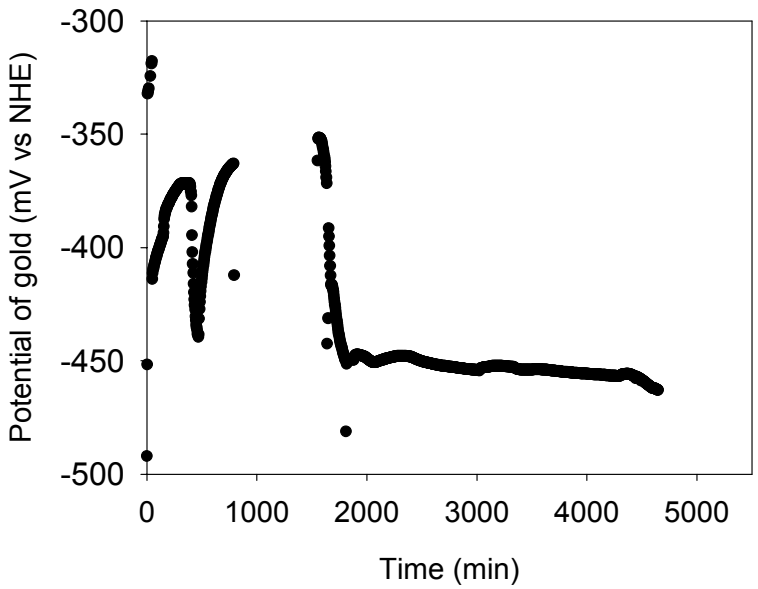

Figure 5-21. *E_h in Test III after the addition of U to 0.1 M NaCl (initial pH 11) in the presence of iron strips (25°C).*

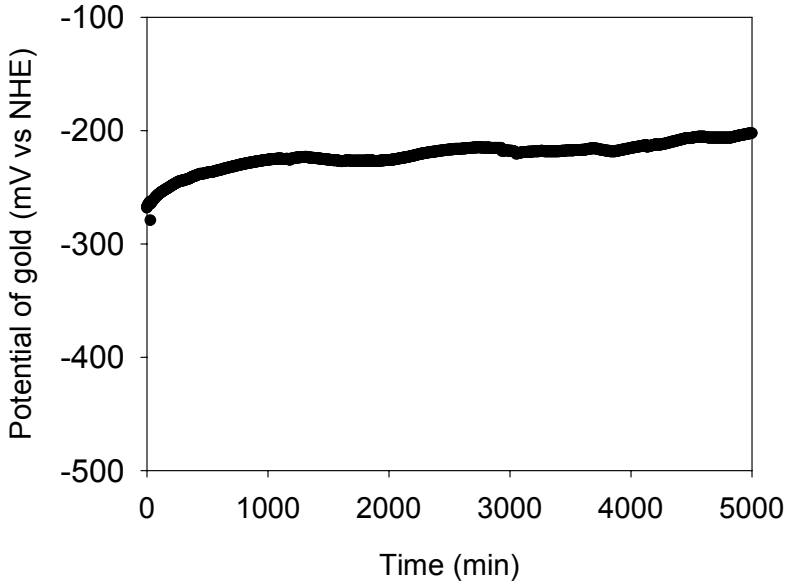

Figure 5-22*. E_h in Test IV after the addition of U to 0.1 M NaCl (initial pH 11) in the presence of iron strips (25°C).*

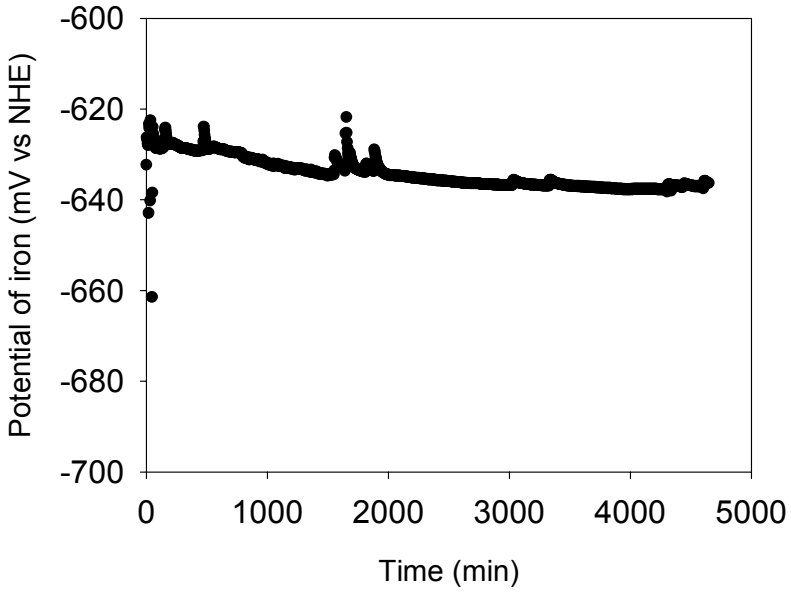

***Figure 5-23**. Corrosion potential of iron in Test III after the addition of U to 0.1 M NaCl (initial pH 11) in the presence of iron strips (25°C).*

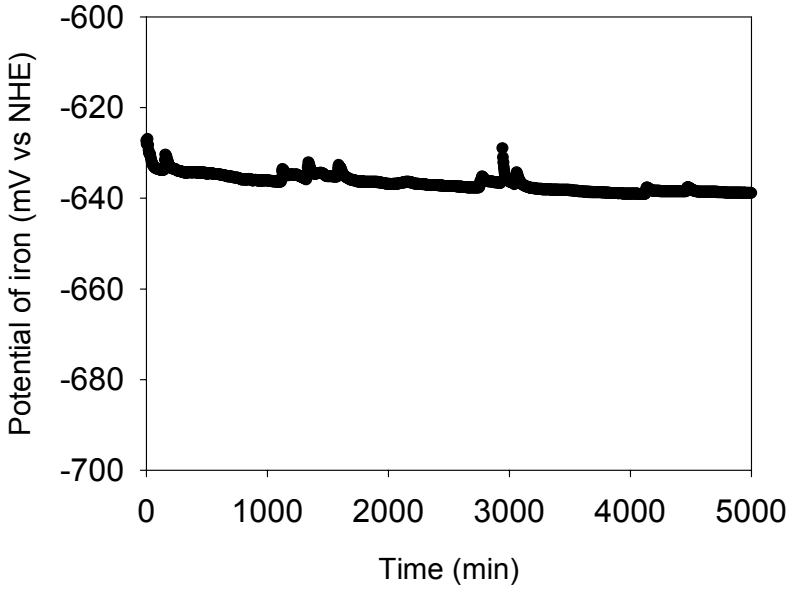

***Figure 5-24**. Corrosion potential of iron in Test IV after the addition of U to 0.1 M NaCl (initial pH 11) in the presence of iron strips (25°C).*

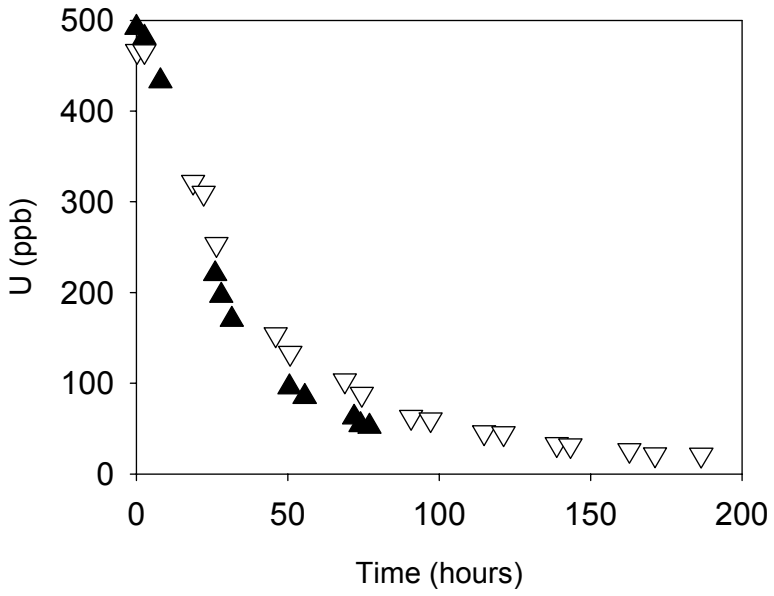

Figure 5-25*. Total U concentration (ppb) in Test III (black symbols) and Test IV (open symbols) after the addition of U to 0.1 M NaCl (initial pH 11) in the presence of iron strips (25°C).*

7 Conclusions

The RIXS measurements show that at least partial reduction of both uranyl carbonate complexes and neptunyl carbonate complexes take place on the corroding iron surface.

The chemical/electrochemical measurements indicate that reduction of uranyl carbonate complexes also take place in solution in a system containing corroding iron, i.e. sorption onto the iron/iron oxide surface may not be necessary in order for reduction to take place. Reduction of uranyl hydroxyl complexes was also found to take place in solution, but at a rate that was noticeably lower than for the uranyl carbonate complexes.

Acknowledgements

D.K. Shuh's and J-H Guo's (Lawrence Berkeley National Laboratory) contributions to make the work at the Advanced Light Source successful are greatly appreciated. Important contributions to the RIXS studies were also made by K. Kvashnina and I.L. Soroka (Uppsala University) and K.E. Roberts (Lawrence Livermore National laboratory).

We thank Posiva, SKB and European commission for funding this project.

References

1. **Butorin S M, 2000.** *J. Electr. Spectros. Rltd. Phenomena* 110–111, 213.

2. **Vuorinen U, Snellman M, 1998.** Finnish reference waters for solubility, sorption and diffusion studies. Helsinki, Finland: Posiva Oy. Posiva Working Report 98–61.

3. **Kalkowski G, Kaindl G, Brewer W D, Krone W, 1987.** *Phys. Rev.* B35, 2667.

4. **Warwick T, Heimann P, Mossessian D, McKinney W, Padmore H, 1995.** *Rev. Sci. Instrum.* 66, 2037.

5. **Gruber J B, Menzel E R, 1969.** *J. Chem. Phys*. 50 3772.

6. **Jørgensen C K, 1955.** *J. Inorg. Nucl. Chem*. 1 301.

7. **Ollila K, 1996.** "Determination of U oxidation state in anoxic (N_2) aqueous solutions – method development and testing", Helsinki, Finland: Posiva Oy. Posiva Report 96-01.

8. **Peat R, Brabon S, Smart N R, 2001.** "Design of Active Corrosion Cell", Serco Assurance Report SA/RJCB/62035/R01 Issue 1.

ISSN 1404-0344

CM Digitaltryck AB, Bromma, 2003